

Finite-Component Multicriticality at the Superradiant Quantum Phase Transition

Han-Jie Zhu,¹ Kai Xu,¹ Guo-Feng Zhang^{1,*} and Wu-Ming Liu^{2,3,4}

¹Key Laboratory of Micro-Nano Measurement-Manipulation and Physics (Ministry of Education), School of Physics, Beihang University, Xueyuan Road No. 37, Beijing 100191, China

²Beijing National Laboratory for Condensed Matter Physics, Institute of Physics, Chinese Academy of Sciences, Beijing 100190, China

³School of Physical Sciences, University of Chinese Academy of Sciences, Beijing 100190, China

⁴Songshan Lake Materials Laboratory, Dongguan, Guangdong 523808, China



(Received 28 February 2020; accepted 8 July 2020; published 28 July 2020)

We demonstrate the existence of finite-component multicriticality in a qubit-boson model where biased qubits collectively coupled to a single-mode bosonic field. The interplay between biases and boson-qubit coupling produces a rich phase diagram which shows multiple superradiant phases and phase boundaries of different orders. In particular, multiple phases become indistinguishable in appropriate bias configurations, which is the signature of multicriticality. A series of universality classes characterizing these multicritical points are identified. Moreover, we present a trapped-ion realization with the potential to explore multicritical phenomena experimentally using a small number of ions. The results open a novel way to probe multicritical universality classes in experiments.

DOI: [10.1103/PhysRevLett.125.050402](https://doi.org/10.1103/PhysRevLett.125.050402)

Quantum multicriticality, where multiple phases simultaneously become identical at a specific quantum critical point, is a fascinating phenomenon as well as fundamental concept in the study of quantum phase transitions [1]. At a multicritical point, the system is governed by a new universality class, which results in qualitatively different critical behaviors including new scaling fields and critical exponents [2]. Owing to this unique nature, intriguing features and novel universality classes have been found in various multicritical systems, including magnetic materials [3], superconductors [4], optical systems [5], and various condensed matter systems [6–15].

Despite the novelty and significance, the investigation of quantum multicriticality is still very limited due to enormous challenges in experiments. To reach a high-order critical point, multiple parameters need to be fine-tuned precisely, e.g., accurate adjustments of composition and magnetic field are both required to access the tricritical point in $\text{Nb}_{1-y}\text{Fe}_{2+y}$ [16]. This imposes a much stricter requirement on the controllability of actual systems compared to normal critical cases [16–18]. Furthermore, while universality class plays a central role in multicritical phenomena, its exploration is even more difficult since universal behavior emerges only when the system size is sufficiently large, and such behavior is vulnerable to environmental noises owing to the long preparation time of the ground state caused by the critical slowing down. To reveal a universality class, we need to maintain the controllability of a large-size system while preserving universal behavior from noise effects, which is extremely difficult in realistic settings [19].

Instead of entering the large-size limit, a finite-component system may also undergo a quantum phase transition (QPT)

if the thermodynamic limit can be reached in an alternative way. This is the case for the Dicke model [20–35], which describes a bosonic mode collectively coupled to multiple qubits. In this model, a second-order QPT appears when the ratio of the mode frequency to the qubit transition frequency approaches zero [36–38]. This model can be realized in different systems ranging from ultracold atoms [39–44] to superconducting circuits [45–48], where some of them, e.g., trapped-ion systems, have shown the possibility of achieving a finite-component QPT due to its excellent controllability in the required critical regime [49–53]. For such systems, an interesting question arises: can multicriticality be induced while maintaining the system size small? If so, this would be highly desirable since it enables the study of multicriticality in a system with sufficient controllability and noise suppression ability due to small system size. More interestingly, is it possible to explore universality classes through probing the critical behavior under realistic conditions?

In this Letter, we show the existence of quantum multicritical points in a finite-component qubit-boson model via engineering qubit biases. We show that qubit biases can introduce novel features in the phase diagram, and multicritical points emerge in certain bias configurations. These points can be characterized by a series of multicritical universality classes. Critical exponents and scaling relations describing these universality classes are also obtained. Finally, we consider a trapped-ion realization with the potential to explore multicritical phenomena experimentally using a small number of ions. The numerical results show that it is possible to correctly reveal universality classes at multicritical points by nonequilibrium universal functions even with noise effects.

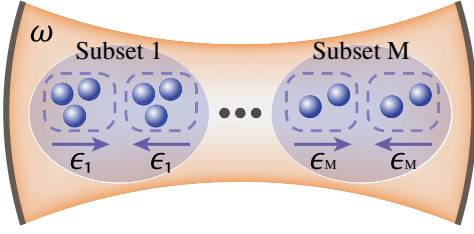


FIG. 1. A schematic illustration of the qubit-boson model with staggered bias configuration [Eq. (1)]. Here a bosonic field with frequency ω is collectively coupled to $2N$ qubits (blue spheres) which are separated into M subsets. Within each subset, qubits are divided into two halves and each half experiences a transverse field with the same magnitude and opposite direction to the other.

Model and phase diagram.—We consider a model that features a rich phase diagram with finite-component multicritical phenomena. The considered system consists of a bosonic field coupled to qubits with a staggered bias configuration (Fig. 1), characterized by the Hamiltonian ($\hbar = 1$)

$$H = \omega a^\dagger a + \sum_{j=1}^M \left[\frac{\Omega}{2} (J_{z,2j-1} + J_{z,2j}) + \frac{\epsilon_j}{2} (J_{x,2j-1} - J_{x,2j}) \right] + \frac{g}{\sqrt{2N}} \sum_{j=1}^M (J_{x,2j-1} + J_{x,2j}) (a^\dagger + a), \quad (1)$$

where a^\dagger (a) is the creation (annihilation) operator of the bosonic field with frequency ω . Here $2N$ qubits are split into M subsets, and for each subset qubits are further divided into two halves which are equipped with biases with the same magnitude (ϵ_j for the j th subset with qubit number $2N_j$) but opposite signs. The collective spin operators $\mathbf{J}_{2j-1} = \sum_{i=1}^{N_j} \boldsymbol{\sigma}_j^{(i)}/2$ and $\mathbf{J}_{2j} = \sum_{i=1}^{N_j} \boldsymbol{\sigma}_j^{(N_j+i)}/2$ are composed of the Pauli operators $\boldsymbol{\sigma}_j^{(i)}$ describing the i th qubit within the j th subset, Ω and g are the energy spacing of qubits and qubit-boson interaction strength, respectively. In the absence of biases, the system returns to the original Dicke model and undergoes a second-order QPT in the $\omega/\Omega \rightarrow 0$ or $N \rightarrow \infty$ limit [36]. With the staggered biases, the system possesses a \mathbb{Z}_2 symmetry associated with the parity transformation $(a, J_{x,2j-1}, J_{x,2j}) \rightarrow (-a, -J_{x,2j}, -J_{x,2j-1})$. The biases can be introduced in various realizations of the Dicke model, e.g., by applying effective transverse Zeeman fields to atoms or ions systems [54], or tuning the persistent currents in superconducting qubits [47].

The biases can introduce important novel features in the phase diagram. To investigate the phase structure, we first resort to the mean-field (MF) approach and the ground-state properties can be analyzed by minimizing the energy functional per qubit (see the Supplemental Material [55] for details)

$$E(z) = \frac{z^2}{4\tilde{g}^2} - \frac{1}{4} \sum_{j=1}^M n_j \left(\sqrt{(z + \tilde{\epsilon}_j)^2 + 1} + \sqrt{(z - \tilde{\epsilon}_j)^2 + 1} \right) \quad (2)$$

where $n_j = N_j/N$ is the number fraction of the j th subset, $\tilde{g} = 2g/\sqrt{\omega\Omega}$ and $\tilde{\epsilon}_j = \epsilon_j/\Omega$ are the dimensionless coupling strength and bias, respectively, and $z = 2\sqrt{\eta}\tilde{g}\varphi$ is the rescaled order parameter characterizing the superradiant transition where $\varphi = \langle a \rangle$ and $\eta = (2N\Omega)^{-1}\omega$ are the bosonic coherence and frequency ratio, respectively. The superradiant QPT is marked by a transition from normal phase (NP) ($\varphi = 0$) to superradiant phase (SP) ($\varphi \neq 0$) accompanied by the \mathbb{Z}_2 symmetry breaking, and the corresponding critical points form a manifold in the parameter space. In this manifold, multicritical points of at most $(M + 2)$ th order can arise, which can be shown by expanding $E(z)$ up to $(2M + 4)$ th order of z as $E(z) = E_0 + v(rz^2/2 + \sum_{j=1}^M u_j z^{2(j+1)}/(2j+2) + z^{2(M+2)}/(2M+4))$. For appropriate $\{n_j\}$ settings, it is possible that the coefficients r and u_1, \dots, u_M vanish simultaneously since there exists $M + 1$ independent parameters \tilde{g} and $\{\tilde{\epsilon}_j\}$. This point is nothing but an $(M + 2)$ th order critical point if it further satisfies $v > 0$. For a complete description of this multicritical point, we further introduce symmetry-breaking biases $H_{ns} = \sum_j h_j (J_{x,2j-1} + J_{x,2j})/2$ to the Hamiltonian. The resulting energy functional $E_{ns}(z)$ can be expanded as $E_{ns}(z) = E(z_{ns}) + v \sum_{j=1}^{M+1} w_j z_{ns}^{2j-1}/(2j-1)$ up to $O(\tilde{h}_j)$, where $\tilde{h}_j = h_j/\Omega$ and $z_{ns} = z - z_0$ with the constant z_0 chosen to remove the z_{ns}^{2M+3} term [55]. Then at this critical point, r , $\{u_j\}$ and $\{w_j\}$ form a complete set of scaling variables, and the critical behavior can be described in terms of these variables.

The simplest $M = 1$ case permits the appearance of tricritical points (TCPs). Figure 2(a) presents the extended phase diagram in the parameter space $(\tilde{g}, \tilde{\epsilon}, \tilde{h})$ (subscripts of $\tilde{\epsilon}_1$ and \tilde{h}_1 are omitted in this case). Here the second-order critical line L_λ turns into a triple line L_τ where three phases coexist as the bias $\tilde{\epsilon}$ is strong enough, and their meeting point additionally connects to two wing critical lines L_\pm . The critical lines L_λ and L_\pm further connect to the coexistence surfaces S_0 and S_\pm , respectively. These structures are the signatures of tricriticality [56], and the meeting point is a TCP whose location can be determined by $u = r = 0$, i.e., $(\tilde{g}_T, \tilde{\epsilon}_T) = [(5/4)^{3/4}, 1/2]$. The occurrence of tricriticality can also be observed through the ground state order parameter, as shown in Fig. 2(b). Clearly, the tricriticality causes a bifurcation of the first-order surfaces S_0 into two wings S_\pm ending at L_\pm .

The next case $M = 2$ allows the existence of tetracritical points (TECPs) where four phases become identical simultaneously, as shown in Figs. 2(c) and 2(d) which illustrate the phase diagram and the corresponding order parameter z_G for fixed $\tilde{\epsilon}_2$, respectively. When $\tilde{\epsilon}_2$ is small, two pairs of SPs arise with a low or high bosonic coherence. Such a difference in superradiant properties indicates that the interplay between biases and boson-qubit coupling induces different collective behaviors of qubits. Moreover, a

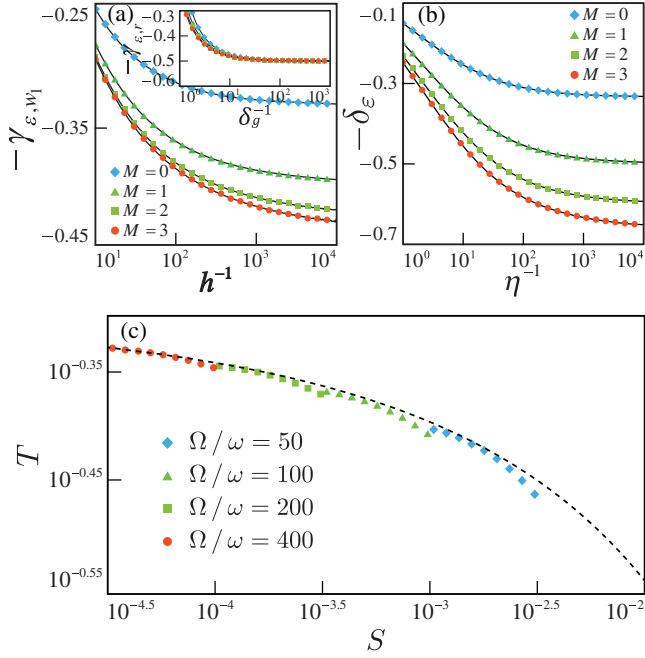


FIG. 3. (a) Fits of the critical exponents γ_{ϵ, w_1} and $\gamma_{\epsilon, r}$ [inset of (a)] at critical points of different orders. (b) Fits of the critical exponent δ_ϵ . (c) Numerical results of the rescaled residual qubit population $S = \eta^{-1+\gamma_{\epsilon, r}/\xi_r} \langle J_z \rangle_r = \sqrt{2}(\omega/\Omega)^{-1/2} \langle J_z \rangle_r$ after quench as a function of the rescaled quench time $T = \omega\tau\eta^{(1+\gamma_{\epsilon, r})/\xi_r} = 2^{-3/2}(\omega/\Omega)^{3/2}\omega\tau$ for different frequency ratio with noise effects included. The black dashed line is the nonequilibrium scaling function \mathcal{S}_{J_z} obtained in the $\eta \rightarrow 0$ limit numerically.

$\delta_\epsilon = \gamma_{\epsilon, r}/\xi_r = \gamma_{\epsilon, w_1}/\xi_{w_1}$ is the finite-frequency scaling exponent, and $\xi_r = (M+3)/(2M+2)$, $\xi_{w_1} = (M+3)/(2M+3)$ are observable-independent exponents which are specific to the universality class [Fig. 3(b)] [55]. Apparently, multicritical points with different orders do indeed belong to different universality classes with distinct scaling fields and critical exponents. These classes are the extensions of the Dicke universality class $M = 0$ in the multicritical regime.

Experimental realization.—Instead of the equilibrium approach, we explore the universality of multicritical points via nonequilibrium scaling functions arising from near adiabatic quenching. Such functions are more robust than equilibrium scaling functions under environmental noises due to lower time requirement [49,57,58]. Therefore, we consider a linear quench $\tilde{g}(t) = \tilde{g}_{(M)}t/\tau$ from $t = 0$ to $t = \tau$ in the symmetry case while fixing the biases $\tilde{e}_j = \tilde{e}_{j,(M)}$, where τ is the duration of quench. The system is initially prepared in the ground state, and we focus on the residual qubit population $\langle J_z \rangle_r \equiv |\langle J_z \rangle_f(\eta, \tau) - \langle J_z \rangle(\eta)|$ at the end of the quench since $\langle J_z \rangle$ can be measured with high fidelity in the trapped-ion setup [50]. Here $\langle J_z \rangle_f(\eta, \tau)$ and $\langle J_z \rangle(\eta)$ denote the expectation value of J_z after quench and that of the ground state when $t = \tau$, respectively. For large enough τ , the adiabatic condition can be satisfied outside the critical regime during quenching, and failed only near the critical

point. Thus the majority of excitations are produced during the nonadiabatic quench inside the critical regime, and $\langle J_z \rangle_r$ satisfies a scaling relation [55]

$$\langle J_z \rangle_r = \eta^{1-\gamma_{\epsilon, r}/\xi_r} \mathcal{S}_{J_z}(\tau\eta^{(1+\gamma_{\epsilon, r})/\xi_r}), \quad (3)$$

where \mathcal{S}_{J_z} is the nonequilibrium scaling function. If $\eta^{-1+\gamma_{\epsilon, r}/\xi_r} \langle J_z \rangle_r$ is plotted as a function of $\tau\eta^{(1+\gamma_{\epsilon, r})/\xi_r}$, all data points with different η should collapse to a single curve, which allows us to determine the order of a critical point and reveal its universality class via ξ_r .

This approach is possible in experiments. For simplicity, we focus on the tricritical case, and consider an experimental realization comprised of two trapped ions which are cooled down to their motional ground states. Here qubits are encoded using different electronic states [59], while the bosonic field is the center-of-mass vibrational mode supported by the Coulomb repulsion and confining potentials [60]. The qubit biases can be generated by additional near-resonant lasers [54]. Finally, the spin-phonon coupling is induced by a pair of laser beams with frequencies slightly detuned from the red and blue sidebands, respectively [50,54,61]. In this setup, the system can be described by an effective Hamiltonian which has the desired form Eq. (1) with $N = M = 1$, and the parameters associate with the experimental ones as $\omega = (\delta_b - \delta_r)/2$, $\Omega = (\delta_b + \delta_r)/2$, $g = \sqrt{2}\eta_0\Omega_0$ and $\epsilon = \Omega_p$ [55]. Here δ_b (δ_r) is the detuning to the blue (red) sidebands, Ω_0 and η_0 are the Rabi strength and Lamb-Dicke parameter of the blue (red)-sideband lasers, respectively, and Ω_p is the Rabi strength of the laser which produces staggered biases. For typical trapped-ion platforms, it is possible to achieve $\omega = (2\pi)200$ Hz and frequency ratios $50 \leq \Omega/\omega \leq 400$ [59]. To reach the tricritical point, it is necessary to realize the Rabi frequencies $9.9 \leq \Omega_0/(2\pi) \leq 27.9$ kHz and $5.0 \leq \Omega_p/(2\pi) \leq 40.0$ kHz ($\eta_0 = 0.06$ is considered), which are attainable in experiment [59].

We now evaluate whether the scaling function can be correctly retrieved when noise effects are taken into account. Here we only consider phonon heating as the main noise source since the qubit dephasing produced by the magnetic-field fluctuations can be effectively suppressed via continuous dynamical decoupling [62–64], and the qubit decay is much slower than the phonon heating rate (~ 1 s qubit lifetime vs ~ 100 ms phonon coherence time) [65]. Then the quench process is governed by a phenomenological master equation $\dot{\rho} = -i[H(\tilde{g}(t)), \rho] + \gamma(n_{\text{th}} + 1)\mathcal{D}[a] + \gamma n_{\text{th}}\mathcal{D}[a^\dagger]$ where $\mathcal{D}[A] = A\rho A^\dagger - \{\rho, A^\dagger A\}/2$, γ is the phonon-reservoir coupling strength and n_{th} is the mean phonon number when the system is in equilibrium with the reservoir. The phonon heating rate is set to a typical value $\gamma n_{\text{th}}/\omega = 0.05$ and the effective temperature of the reservoir is high enough such that $\gamma n_{\text{th}} \approx \gamma(n_{\text{th}} + 1)$. Figure 3(c) shows the quench results of $\langle J_z \rangle_r$ with the noise effects, where the quench time is chosen in a range $0.75 \leq \omega\tau \leq 2$ ($3.75 \leq \tau \leq 10$ ms) which is much

shorter than the phonon coherence time. We can find that all data points with different η collapse into a theoretical line of \mathcal{S}_{J_z} approximately, thus the scaling function \mathcal{S}_{J_z} can be faithfully retrieved under environmental noises. This allows the identification of multicritical universality classes.

Conclusion.—In conclusion, we have shown that finite-component multicriticality can be induced by the interplay between qubit biases and boson-qubit coupling. In certain bias configurations, multiple phases become indistinguishable and this relates to a high-order critical point which resides between a multiple coexistence line and a lower-order critical line in the phase diagram. These points can be characterized by a series of multicritical universality classes. Moreover, we have presented a trapped-ion realization with the potential to explore multicritical phenomena experimentally. Because of the small system size, we are able to retain necessary controllability and coherence under realistic conditions, thus making it possible for experiments to reveal the multicritical universality classes through nonequilibrium universal functions. Our work extends the multicriticality study to finite-component systems, and thus opens a new way of studying multicritical phenomena and provides a promising platform for experimental exploration.

This work was supported by NSFC under Grants No. 11574022, No. 61835013, No. 61227902, No. 61721091, the National Key R&D Program of China under Grant No. 2016YFA0301500, Strategic Priority Research Program of the Chinese Academy of Sciences under Grants No. XDB01020300 and No. XDB21030300.

H. J. Z. and G. F. Z. contributed equally to this work.

*gf1978zhang@buaa.edu.cn

- [1] S. Sachdev, *Quantum Phase Transitions*, 2nd ed. (Cambridge University Press, Cambridge, England, 2011).
- [2] J. Cardy, *Scaling and Renormalization in Statistical Physics*, Cambridge Lecture Notes in Physics (Cambridge University Press, Cambridge, England, 1996).
- [3] Y. Kato and T. Misawa, *Phys. Rev. B* **92**, 174419 (2015).
- [4] G. Giovannetti, C. Ortix, M. Marsman, M. Capone, J. V. Den Brink, and J. Lorenzana, *Nat. Commun.* **2**, 398 (2011).
- [5] Y. Xu and H. Pu, *Phys. Rev. Lett.* **122**, 193201 (2019).
- [6] S. Yin, S.-K. Jian, and H. Yao, *Phys. Rev. Lett.* **120**, 215702 (2018).
- [7] G. I. Martone, F. V. Pepe, P. Facchi, S. Pascazio, and S. Stringari, *Phys. Rev. Lett.* **117**, 125301 (2016).
- [8] Y. Kato, D. Yamamoto, and I. Danshita, *Phys. Rev. Lett.* **112**, 055301 (2014).
- [9] G. Ceccarelli, J. Nespolo, A. Pelissetto, and E. Vicari, *Phys. Rev. A* **93**, 033647 (2016).
- [10] B. Roy and M. S. Foster, *Phys. Rev. X* **8**, 011049 (2018).
- [11] B. Roy and V. Juricic, *Phys. Rev. B* **99**, 241103(R) (2019).
- [12] B. Roy, P. Goswami, and V. Juričić, *Phys. Rev. B* **97**, 205117 (2018).
- [13] X. Luo, B. Xu, T. Ohtsuki, and R. Shindou, *Phys. Rev. B* **97**, 045129 (2018).
- [14] J. Leonard, A. Morales, P. Zupancic, T. Esslinger, and T. Donner, *Nature (London)* **543**, 87 (2017).
- [15] A. Morales, P. Zupancic, J. Leonard, T. Esslinger, and T. Donner, *Nat. Mater.* **17**, 686 (2018).
- [16] S. Friedemann, W. J. Duncan, M. Hirschberger, T. Bauer, R. Kuchler, A. Neubauer, M. Brando, C. Pfleiderer, and F. M. Grosche, *Nat. Phys.* **14**, 62 (2018).
- [17] Y. Tokunaga, D. Aoki, H. Mayaffre, S. Krämer, M.-H. Julien, C. Berthier, M. Horvatić, H. Sakai, S. Kambe, and S. Araki, *Phys. Rev. Lett.* **114**, 216401 (2015).
- [18] F. Wu, C. Y. Guo, Y. Chen, H. Su, A. Wang, M. Smidman, and H. Q. Yuan, *Phys. Rev. B* **99**, 064419 (2019).
- [19] D. Suter and G. A. Álvarez, *Rev. Mod. Phys.* **88**, 041001 (2016).
- [20] R. H. Dicke, *Phys. Rev.* **93**, 99 (1954).
- [21] V. M. Bastidas, C. Emary, B. Regler, and T. Brandes, *Phys. Rev. Lett.* **108**, 043003 (2012).
- [22] M. Oriente, T. Donner, R. Chitra, and O. Zilberberg, *Phys. Rev. Lett.* **120**, 183603 (2018).
- [23] P. Kirton, M. M. Roses, J. Keeling, and E. G. Dalla Torre, *Adv. Quantum Technol.* **2**, 1970013 (2019).
- [24] X. Y. Lü, L. L. Zheng, G. L. Zhu, and Y. Wu, *Phys. Rev. Applied* **9**, 064006 (2018).
- [25] H. J. Zhu, G. F. Zhang, L. Zhuang, and W. M. Liu, *Phys. Rev. Lett.* **121**, 220403 (2018).
- [26] J. Peng, E. Rico, J. Zhong, E. Solano, and I. L. Egusquiza, *Phys. Rev. A* **100**, 063820 (2019).
- [27] J. P. J. Rodriguez, S. A. Chilingaryan, and B. M. Rodríguez-Lara, *Phys. Rev. A* **98**, 043805 (2018).
- [28] Y. Alavirad and A. Lavasani, *Phys. Rev. A* **99**, 043602 (2019).
- [29] S. Ashhab, Y. Matsuzaki, K. Kakuyanagi, S. Saito, F. Yoshihara, T. Fuse, and K. Semba, *Phys. Rev. A* **99**, 063822 (2019).
- [30] L. Garbe, I. L. Egusquiza, E. Solano, C. Ciuti, T. Coudreau, P. Milman, and S. Felicetti, *Phys. Rev. A* **95**, 053854 (2017).
- [31] S. Felicetti and A. Le Boité, *Phys. Rev. Lett.* **124**, 040404 (2020).
- [32] L. Garbe, M. Bina, A. Keller, M. G. A. Paris, and S. Felicetti, *Phys. Rev. Lett.* **124**, 120504 (2020).
- [33] J. Leonard, A. Morales, P. Zupancic, T. Donner, and T. Esslinger, *Science* **358**, 1415 (2017).
- [34] R. M. Kroeze, Y. Guo, V. D. Vaidya, J. Keeling, and B. L. Lev, *Phys. Rev. Lett.* **121**, 163601 (2018).
- [35] A. Morales, D. Dreon, X. Li, A. Baumgärtner, P. Zupancic, T. Donner, and T. Esslinger, *Phys. Rev. A* **100**, 013816 (2019).
- [36] M.-J. Hwang, R. Puebla, and M. B. Plenio, *Phys. Rev. Lett.* **115**, 180404 (2015).
- [37] M.-J. Hwang and M. B. Plenio, *Phys. Rev. Lett.* **117**, 123602 (2016).
- [38] M. Liu, S. Chesi, Z.-J. Ying, X. Chen, H.-G. Luo, and H.-Q. Lin, *Phys. Rev. Lett.* **119**, 220601 (2017).
- [39] K. Baumann, C. Guerlin, F. Brennecke, and T. Esslinger, *Nature (London)* **464**, 1301 (2010).
- [40] M. P. Baden, K. J. Arnold, A. L. Grimsmo, S. Parkins, and M. D. Barrett, *Phys. Rev. Lett.* **113**, 020408 (2014).
- [41] A. Safavi-Naini, R. J. Lewis-Swan, J. G. Bohnet, M. Gärtner, K. A. Gilmore, J. E. Jordan, J. Cohn, J. K. Freericks,

- A. M. Rey, and J. J. Bollinger, *Phys. Rev. Lett.* **121**, 040503 (2018).
- [42] M. Garttner, J. G. Bohnet, A. Safavinaini, M. L. Wall, J. J. Bollinger, and A. M. Rey, *Nat. Phys.* **13**, 781 (2017).
- [43] P. Schneeweiss, A. Dureau, and C. Sayrin, *Phys. Rev. A* **98**, 021801(R) (2018).
- [44] X.-H. Cheng, I. Arrazola, J. S. Pedernales, L. Lamata, X. Chen, and E. Solano, *Phys. Rev. A* **97**, 023624 (2018).
- [45] N. K. Langford, R. Sagastizabal, M. Kounalakis, C. Dickel, A. Bruno, F. Luthi, D. J. Thoen, A. Endo, and L. Dicarlo, *Nat. Commun.* **8**, 1715 (2017).
- [46] J. P. Martinez, S. Leger, N. Gheeraert, R. Dassonneville, L. Planat, F. Foroughi, Y. Krupko, O. Buisson, C. Naud, W. Haschguichard *et al.*, *npj Quantum Inf.* **5**, 19 (2019).
- [47] X. Gu, A. F. Kockum, A. Miranowicz, Y. xi Liu, and F. Nori, *Phys. Rep.* **718–719**, 1 (2017).
- [48] M. Bamba, K. Inomata, and Y. Nakamura, *Phys. Rev. Lett.* **117**, 173601 (2016).
- [49] R. Puebla, M.-J. Hwang, J. Casanova, and M. B. Plenio, *Phys. Rev. Lett.* **118**, 073001 (2017).
- [50] D. Lv, S. An, Z. Liu, J.-N. Zhang, J. S. Pedernales, L. Lamata, E. Solano, and K. Kim, *Phys. Rev. X* **8**, 021027 (2018).
- [51] R. Islam, E. E. Edwards, K. Kim, S. E. Korenblit, C. Noh, H. J. Carmichael, G. D. Lin, L. M. Duan, C. C. J. Wang, J. K. Freericks *et al.*, *Nat. Commun.* **2**, 377 (2011).
- [52] I. Aedo and L. Lamata, *Phys. Rev. A* **97**, 042317 (2018).
- [53] F. M. Gambetta, I. Lesanovsky, and W. Li, *Phys. Rev. A* **100**, 022513 (2019).
- [54] M. L. Wall, A. Safavi-Naini, and A. M. Rey, *Phys. Rev. A* **95**, 013602 (2017).
- [55] See Supplemental Material at <http://link.aps.org/supplemental/10.1103/PhysRevLett.125.050402> for detail explanations and derivations.
- [56] I. Lawrie and S. Sarbach, *Theory of Tricritical Points* (Academic Press, New York, 1984), pp. 1–161.
- [57] O. L. Acevedo, L. Quiroga, F. J. Rodríguez, and N. F. Johnson, *Phys. Rev. Lett.* **112**, 030403 (2014).
- [58] M. M. Rams, J. Dziarmaga, and W. H. Zurek, *Phys. Rev. Lett.* **123**, 130603 (2019).
- [59] R. Gerritsma, G. Kirchmair, F. Zahringer, E. Solano, R. Blatt, and C. F. Roos, *Nature (London)* **463**, 68 (2010).
- [60] D. Porras and J. I. Cirac, *Phys. Rev. Lett.* **92**, 207901 (2004).
- [61] J. S. Pedernales, I. Lizuain, S. Felicetti, G. Romero, L. Lamata, and E. Solano, *Sci. Rep.* **5**, 15472 (2015).
- [62] R. Puebla, J. Casanova, and M. B. Plenio, *New J. Phys.* **18**, 113039 (2016).
- [63] R. Puebla, M. J. Hwang, J. Casanova, and M. B. Plenio, *Phys. Rev. A* **95**, 063844 (2017).
- [64] R. Puebla, J. Casanova, and M. B. Plenio, *J. Mod. Opt.* **65**, 745 (2018).
- [65] F. Schmidt-Kaler, S. Gulde, M. Riebe, T. Deuschle, A. Kreuter, G. P. T. Lancaster, C. Becher, J. Eschner, H. Häffner, and R. Blatt, *J. Phys. B* **36**, 623 (2003).